

Electronic Supplementary Information

**Glutathione-responsive paclitaxel dimer nanovesicles with
high drug content**

Qing Pei,^{a,b} Xiuli Hu,^a Junli Zhou,^{a,b} Shi Liu,^a and Zhigang Xie^a*

^a State Key Laboratory of Polymer Physics and Chemistry, Changchun Institute of Applied Chemistry, Chinese Academy of Sciences

5625 Renmin Street, Changchun, Jilin 130022, P. R. China

E-mail: xiez@ciac.ac.cn; Tel/Fax: 86-431-85262775

^b University of Science and Technology of China, Hefei 230026, P. R. China.

Materials.

Paclitaxel (PTX) was purchased from Xian Haoxuan Biological Technology Co., Ltd.. 1-Ethyl-3-(3-dimethylaminopropyl) carbodiimide hydrochloride (EDC.HCl, GL Biochem), 4-dimethylaminopyridine (DMAP, Aladdin) and 2, 2'-thiodiacetic acid (Aladdin) were used as received. Glutathione (GSH) and Nile red (NR) were both purchased from Shanghai Yuanye Biological Technology Co., Ltd.. Chloroform-d (CDCl_3) was purchased from Qingdao Tenglong Weibo Technology Co., Ltd.. Ultrapure water was prepared from a Milli-Q system (Millipore, USA). Solvents for chemical synthesis were purified by distillation.

Synthesis of PTX-S-PTX.

PTX (200.4 mg, 0.23 mmol) was dissolved in dichloromethane (CH_2Cl_2), and then 2, 2'-thiodiacetic acid (19.9 mg, 0.13 mmol), EDC.HCl (89.8 mg, 0.47 mmol) and DMAP (2.9 mg, 0.024 mmol) were added sequentially. After stirring for 1 h at ambient temperature, additional EDC.HCl (44.9 mg, 0.23 mmol) and DMAP (2.9 mg, 0.024 mmol) were added, and reaction was continued for another 24 h. The reaction product was purified using silica gel column chromatography with CH_2Cl_2 and ethyl acetate to give PTX-S-PTX. Reaction yields were more than 90%. MS (LTQ) m/z: calculated for $\text{C}_{98}\text{H}_{104}\text{N}_2\text{O}_{30}\text{S}$ (PTX-S-PTX) $[\text{M} + \text{Cl}]^-$ 1857.1, found 1856.8.

Preparation of PTX-S-PTX NVs.

PTX-S-PTX NVs were prepared using the nanoprecipitation method. Briefly, 4 mL of PTX-S-PTX (1 mg) solution in tetrahydrofuran (THF) or acetone was injected

into the 10 mL of distilled water at ambient temperature with vigorous stirring. After evaporating organic solvent, the color of the aqueous solution changed into slight blue while nanovesicles were formed. Unincorporated PTX-S-PTX (precipitate) was removed by centrifugation at 5000 rpm for 5 min. The concentration of PTX-S-PTX NVs in solutions was determined through High Performance Liquid Chromatography (HPLC, Shimadzu, CBM-20A) with a UV-vis detector.

Preparation of NR@PTX-S-PTX NVs and ICG@PTX-S-PTX NVs.

The experiment was similar to the preparation of PTX-S-PTX NVs. Add PTX-S-PTX and NR to deionized water to form NR@PTX-S-PTX NVs. ICG@PTX-S-PTX NVs was prepared by adding THF solutions of PTX-S-PTX to aqueous solutions of ICG.

Physicochemical characterization.

Proton nuclear magnetic resonance (^1H NMR) spectra was recorded on a Bruker AV400 M in CDCl_3 at 25 °C. Chemical shifts were given in parts per million from that of tetramethylsilane (TMS) as an internal reference. The mass spectrum (MS) analyses were performed on a LTQ ion trap mass spectrometer (Finnigan, USA) equipped with an electrospray source. Size, size distribution and zeta-potential of the nanovesicles were determined by Malvern Zeta-sizer Nano. The scattering angle was fixed at 90° and the measurement was carried out at 25 °C. The morphology of the nanovesicles was measured by transmission electron microscopy (TEM) performed on a JEOL JEM-1011 electron microscope operating at an acceleration voltage of 100 kV. To prepare specimens for TEM, a drop of nanovesicles solution (0.1 mg/mL) was

deposited onto a copper grid with a carbon coating. The specimens were air-dried and measured at room temperature. Specimens after being air-dried on silicon disk were also measured by scanning electron microscopy (SEM) performed on JEOL JXA-840 under an accelerating voltage of 15 kV. Atomic force microscopy (AFM) characterization of nanovesicles was studied using a SPA-300HV AFM (Japan, Seiko Instruments Inc.) driven in tapping mode. A silicon tip (OLTESPA-R3, Germany, Bruker) with a spring constant of $2 \text{ N}\cdot\text{m}^{-1}$ was used. UV-vis absorption spectra were obtained using a Shimadzu UV-2450 PC UV-vis spectrophotometer. Fluorescence intensity tests were performed using Perkin Elmer LS-55 fluorospectrophotometer. The cellular localization was visualized under a confocal laser scanning microscope (CLSM) (Zeiss LSM 700, Zurich, Switzerland). MTT (3-(4,5-dimethylthiazol-2-yl)-2,5-diphenyltetrazolium bromide) assays were measured at 490 nm by a microplate reader (BioTek, EXL808).

Critical aggregation concentration (CAC) assays.

The critical aggregation concentration (CAC) of PTX-S-PTX NVs was examined using NR probe according to the method as reported in the previous literature.^{1,2}

***In vitro* stability of PTX-S-PTX NVs.**

We utilized fetal bovine serum (FBS) to investigate the stability of PTX-S-PTX NVs by detecting the change of their size and size distribution at 37 °C for different time periods. The ratio of FBS and PBS (pH 7.4) was set as 10/90 (v/v).

Evaluation of crystalline status of PTX, PTX-S-PTX and PTX-S-PTX NVs.

The powder X-ray diffraction (PXRD) was employed to detect the status of PTX

formulations. There were three samples in these tests, including PTX crystal, PTX-S-PTX and freeze-dried powder of PTX-S-PTX NVs. After being fully milled, they were determined by a Bruker D8 Focus power X-ray diffractometer using Cu K α radiation, while the incidence angle 2θ was monitored from 8° to 37°.

GSH-responsive behaviours of PTX-S-PTX NVs and NR@PTX-S-PTX NVs.

(1) DLS measurements: For thiolysis, 10 mM GSH were added to aqueous solution of PTX-S-PTX NVs (25 μ M, 2 mL) under moderate shake at 37 °C. The shake was continued for 2 h, and then the size of reconstructed dispersion was detected by DLS.

(2) Fluorescence measurements: An aqueous dispersion of NR@PTX-S-PTX NVs at concentrations of PTX-S-PTX (94 μ g mL⁻¹) and NR (4.7 μ g mL⁻¹) was incubated with GSH (10 mM) at 37 °C water bath under shake. After 0, 1, 2.5, 6 hours, the reaction mixture was sent for fluorescence measurement to determine the disassembly rate. The excitation wavelength and collecting wavelength of NR@PTX-S-PTX NVs were 520 nm and 636 nm, respectively.

Cell lines and cell culture.

HeLa (human cervical carcinoma), HepG2 (human hepatocellular carcinoma) cell lines were provided by the First Hospital of Jilin University, and grown in Dulbecco's modified Eagle's medium (DMEM, GIBCO) supplemented with 10% heat-inactivated fetal bovine serum (FBS, GIBCO). Cells were cultured in a humidified incubator at 37 °C with 5% CO₂, and the culture medium was replaced once every day.

Cellular uptake measured by CLSM.

The cellular uptake behaviors of NR@PTX-S-PTX NVs were examined by CLSM towards HeLa cells. The cells were seeded in 6-well plates (a clean cover slip was put in each well) at about a density of 200,000 cells per well in 1.5 mL of DMEM medium and allowed to adhere for 24 h. And then the medium was replaced with NR@PTX-S-PTX NVs diluted with fresh culture medium to a final NR concentration of $0.5 \mu\text{g mL}^{-1}$. Thereafter cells were incubated at $37 \text{ }^{\circ}\text{C}$ for additional designed times. Subsequently, the supernatant was removed and the cells were washed gently three times with PBS (pH 7.4), fixed with 4% paraformaldehyde (1 mL/ each well) for 15 min at ambient temperature and washed thrice with cold PBS. DAPI (4',6-diamidino-2-phenyl-indole) was employed to counterstain the cell nuclei. For lysosome colocalization visualization, before the cells were subjected to DAPI, pretreated with Lyso-Tracker Green for 30 min at $37 \text{ }^{\circ}\text{C}$ to stain lysosomes. The cellular uptake was obtained by CLSM, while NR was excited at 555 nm.

Cell viability assays.

The cytotoxicity of various kinds of PTX-S-PTX NVs was examined via MTT protocol with free PTX used as a control. Briefly, HeLa and HepG2 cells harvested in a logarithmic growth phase were seeded in 96-well plates at an initial density of 2×10^3 cells/well and incubated in 100 μL DMEM at $37 \text{ }^{\circ}\text{C}$ in 5% CO_2 atmosphere for overnight. After removing incubation medium, PTX-S-PTX NVs (100 μL) diluted with cell culture media to the desired concentration were added to cell wells at various PTX concentrations from 0.0001 μM to 10 μM . Cells free of PTX-S-PTX NVs and

PTX treatment were used as control. At the specific time intervals (48 h), 20 μL of MTT solution in PBS with the concentration of 5 mg mL^{-1} was added and the plates were incubated at $37 \text{ }^\circ\text{C}$ for another 4 h, straight after careful removal of the culture medium supernatant and addition of $150 \text{ }\mu\text{L}$ of dimethyl sulfoxide (DMSO) to each well to dissolve the formed violet formazan crystals. Finally, the plates were shaken for 3 min, and the absorbance of violet product was quantified at 490 nm by a microplate reader.

***In vitro* PTX release.**

The release rate of PTX from PTX-S-PTX NVs was evaluated as follows: An aqueous dispersion of PTX-S-PTX NVs was cell lysates of HeLa cells. The mixture ($200 \text{ }\mu\text{L}$) was shaken at $37 \text{ }^\circ\text{C}$ in water bath. At designed time, the mixture ($200 \text{ }\mu\text{L}$) was added to acetonitrile (1.4 mL) and centrifuged at 10000 rpm for 10 min. The supernatant was detected by HPLC to determine the hydrolysis rate of the PTX-S-PTX NVs.

***In vivo* bioimaging.**

All experiments were performed in compliance with the guidelines of the Chinese Academy of Science Committee for Animal Use and Care. All experiments followed the NIH guidelines for the care and use of laboratory animals. Chinese Academy of Science Committee approved the animal experiments in this work.

Male nude mice were obtained and maintained under required conditions. All animal procedures were approved and controlled by the local ethics committee and carried out according to the guidelines of Chinese law concerning the protection of

animal life. To evaluate *in vivo* bioimaging of ICG@PTX-S-PTX NVs, subcutaneous human cervical carcinoma HeLa tumor xenografts were utilized as animal model. HeLa cells were subcutaneously inoculated into the lateral aspect of the anterior right limb of mice (5×10^6 cells in 0.1 mL PBS). After the tumor volume reached appropriate size, ICG@PTX-S-PTX NVs were injected into the tumor with the ICG dose of 0.8 mg/kg. At designed time post injection, the mice were imaged by the Maestro in-vivo Imaging System (CRI Maestro™ 2.4, Cambridge Research & Instrumentation, Inc., USA), which consisted of a light-tight box equipped with a 150 W halogen lamp and an excitation filter (671–760 nm) to excite ICG. Fluorescence was detected by a CCD camera equipped with a C-mount lens and an emission filter (750 nm longpass).

Statistical analysis.

Data are presented as the mean \pm standard deviation (SD). One-way analysis of variance (ANOVA) was used to determine significance among groups. Statistical significance was established at $p < 0.05$.

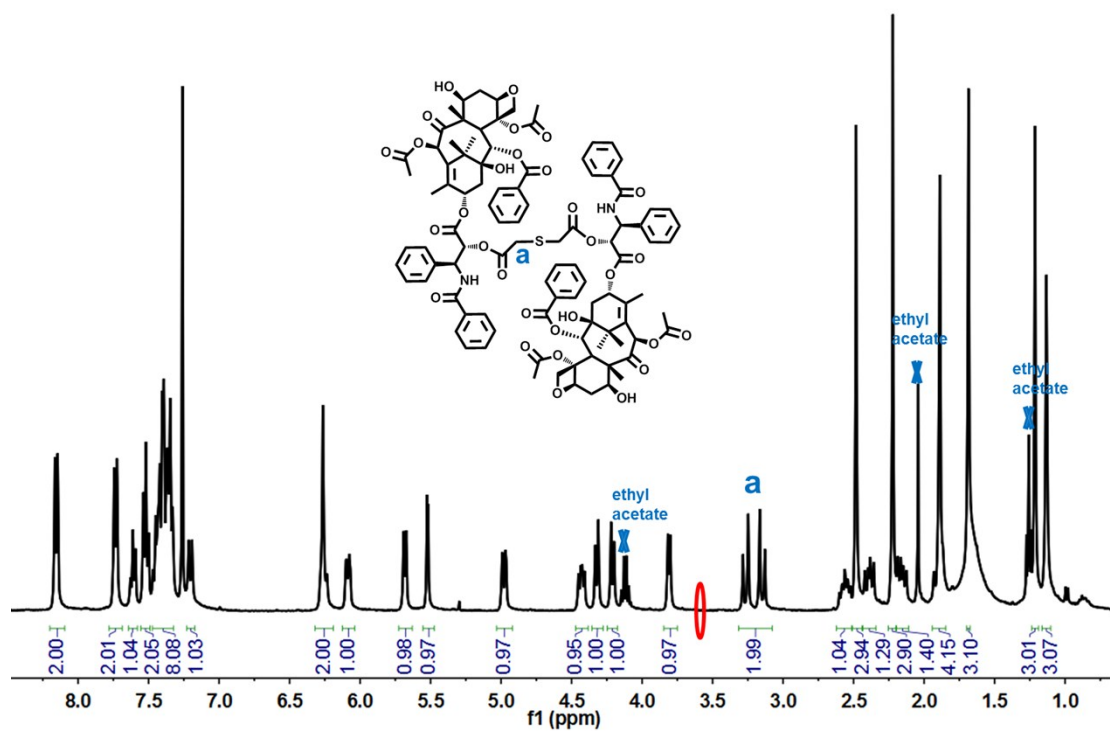


Fig. S1 ^1H NMR spectrum of PTX-S-PTX in CDCl_3 .

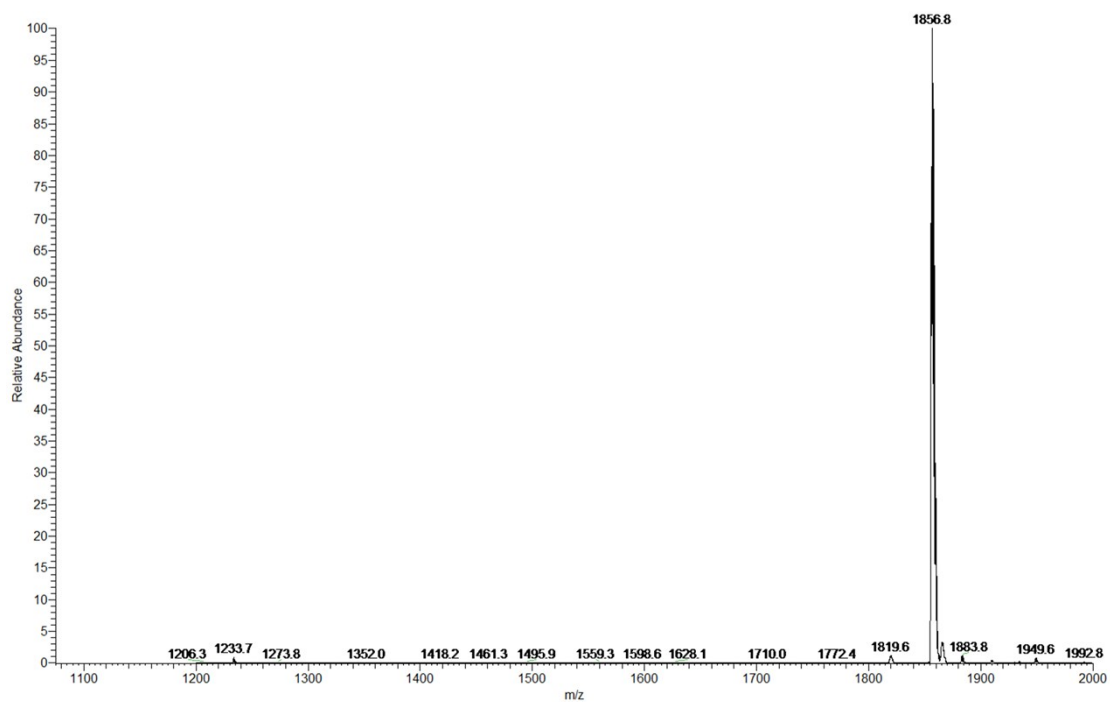


Fig. S2 Mass spectrum of PTX-S-PTX.

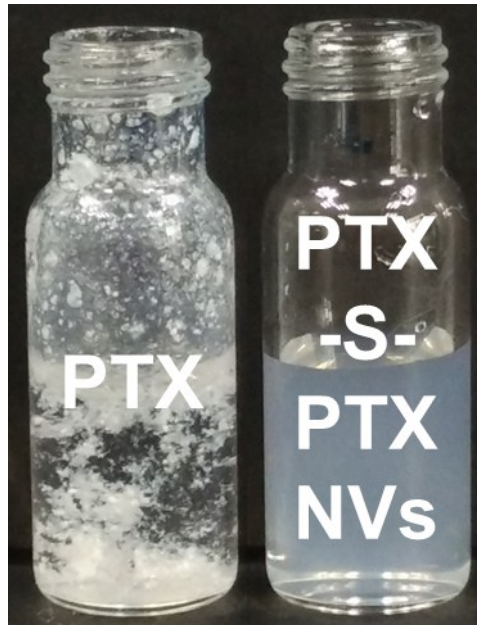


Fig. S3 Dissolution of PTX-S-PTX in water and formation of a clear apparent aqueous dispersions, but PTX tends to precipitate.

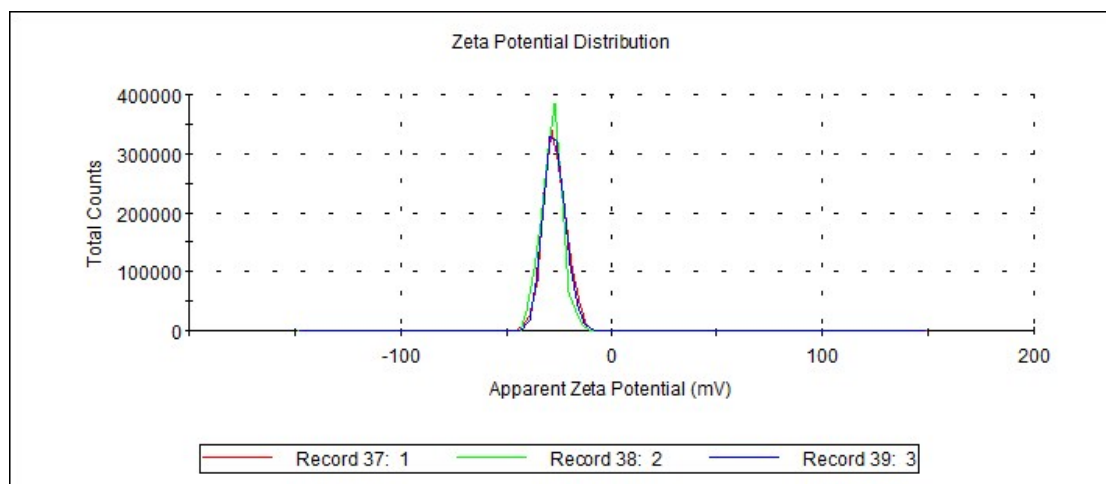


Fig. S4 Zeta potential distribution of PTX-S-PTX NVs.

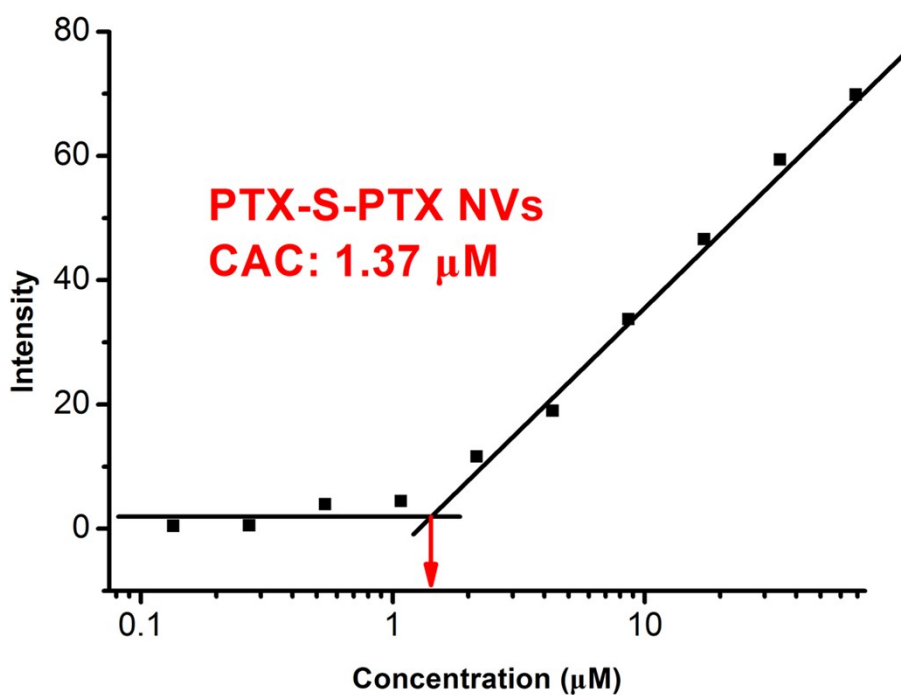


Fig. S5 The critical aggregation concentration (CAC) for PTX-S-PTX NVs.

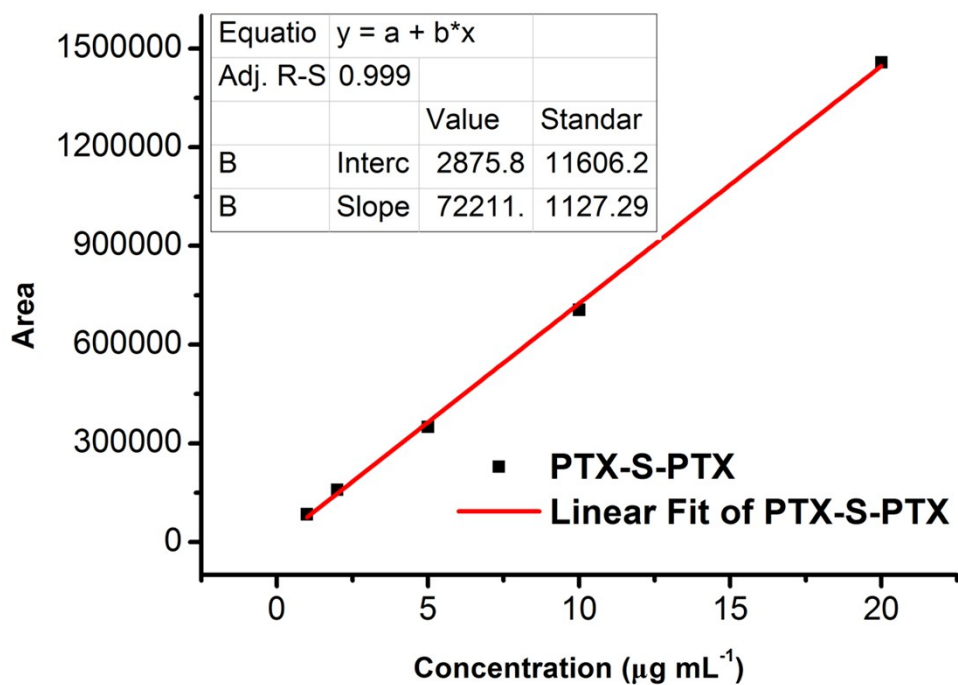


Fig. S6 Standard curve of PTX-S-PTX in acetonitrile by HPLC.

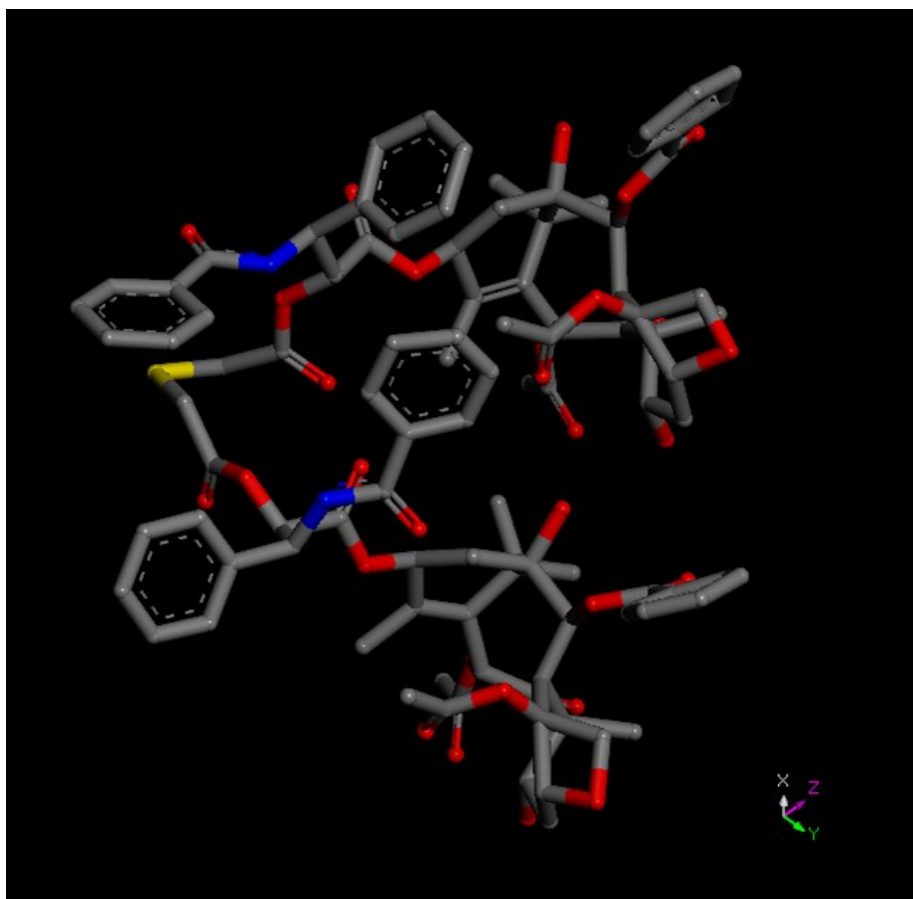


Fig. S7 3D chemical structure of PTX-S-PTX.

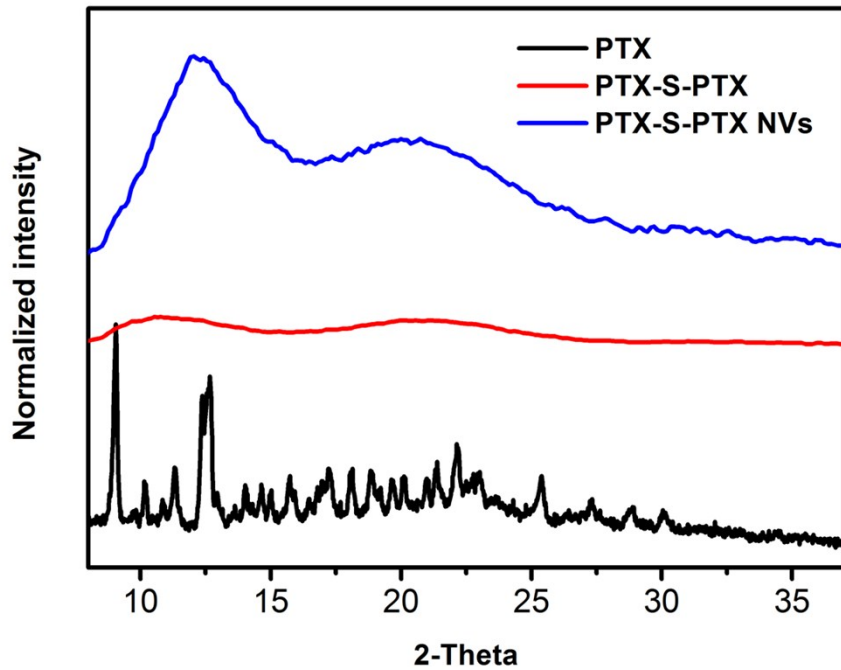


Fig. S8 The powder X-ray diffraction patterns of PTX, PTX-S-PTX and lyophilized powder of PTX-S-PTX NVs.

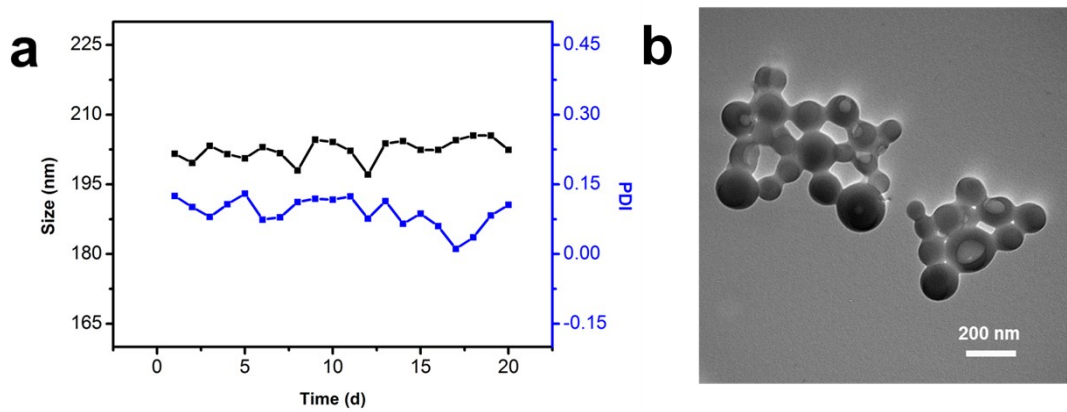


Fig. S9 (a) Change of size and polydispersity index (PDI) of PTX-S-PTX NVs when stored at -4 °C for two weeks. (b) TEM images of PTX-S-PTX NVs after stored for three months.

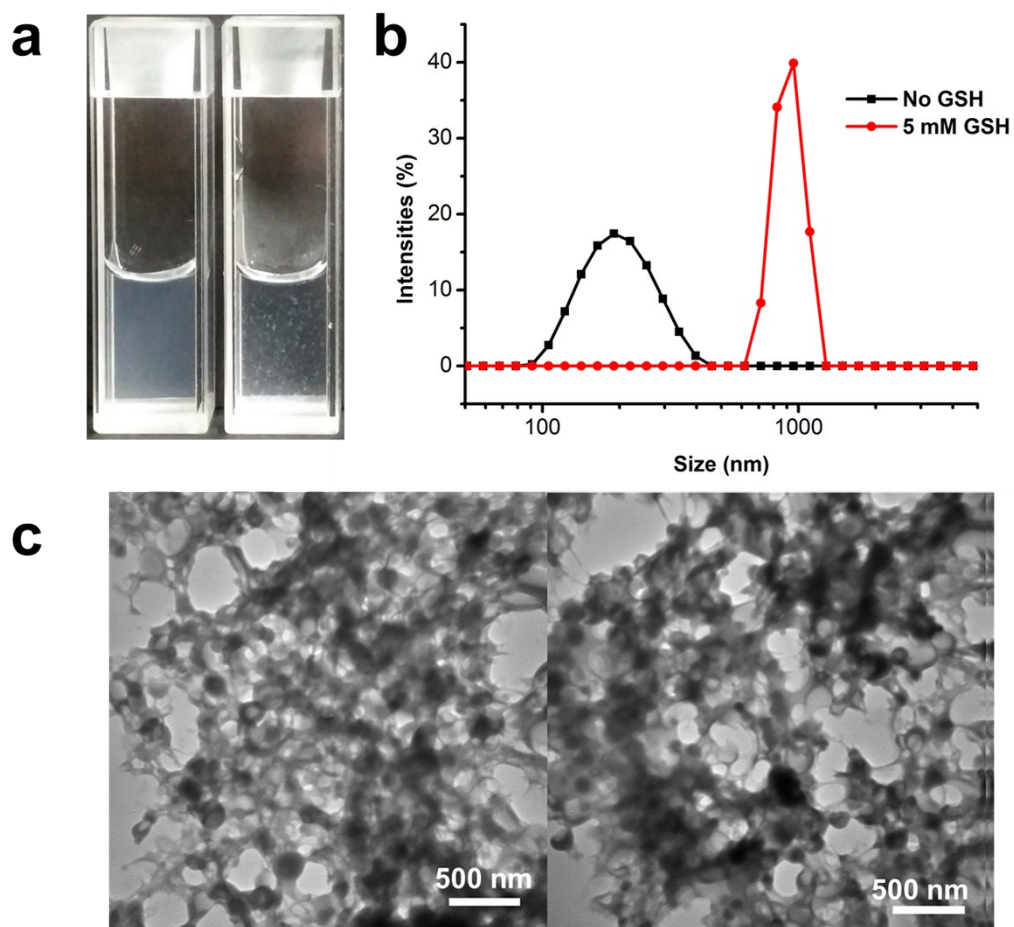


Fig. S10 (a) The photo of PTX-S-PTX NVs solutions before and after 5 mM GSH treatment. (b) GSH-triggered disintegration of PTX-S-PTX NVs evaluated by change of size. (c) TEM images of PTX-S-PTX NVs after 5 mM GSH treatment.

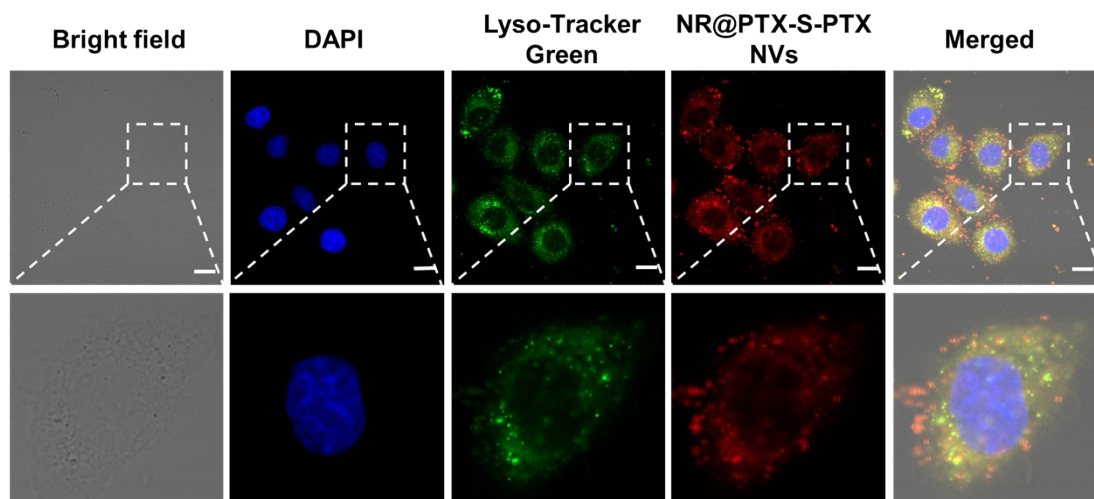


Fig. S11 CLSM images of HeLa cells treated with NR@PTX-S-PTX NVs at 37 °C for 2 h. From left to right: pictures correspond to Bright field, DAPI (blue), Lyso-Tracker Green (green), NR@PTX-S-PTX NVs (red) and merged images. Scale bar, 20 μ m.

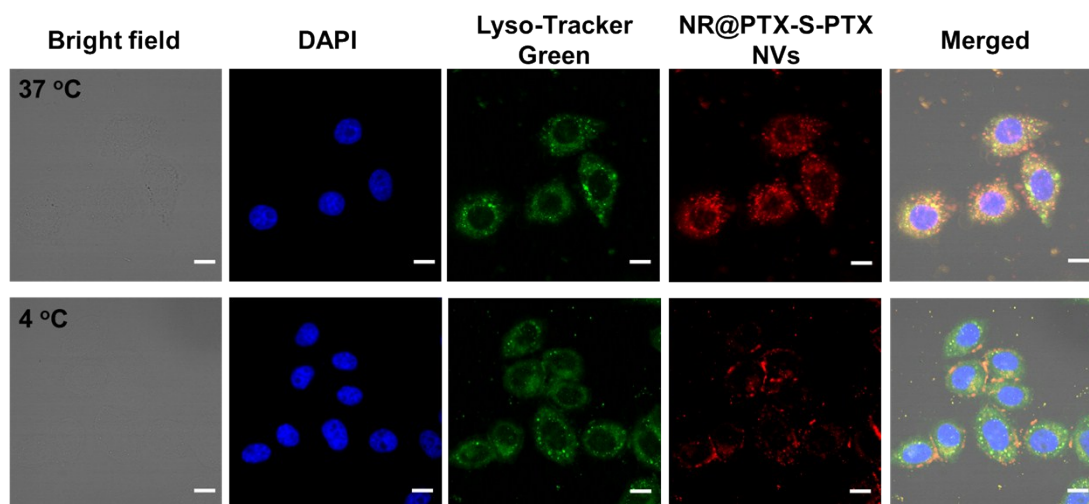


Fig. S12 CLSM images of HeLa cells treated with NR@PTX-S-PTX NVs at 37 °C and 4 °C for 2 h. From left to right: pictures correspond to Bright field, DAPI (blue), Lyso-Tracker Green (green), NR@PTX-S-PTX NVs (red) and merged images. Scale

bar, 20 μm .

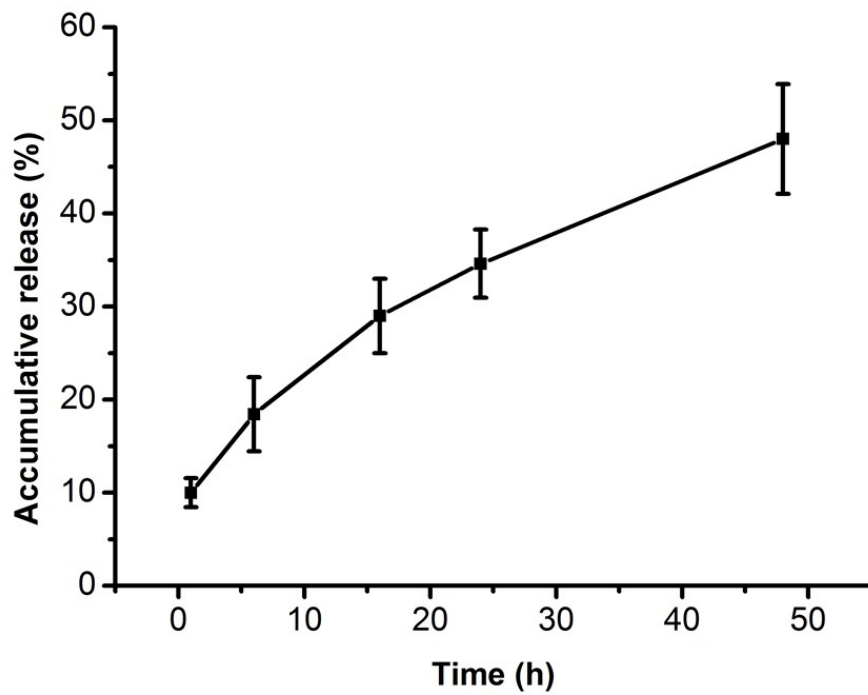


Fig. S13 *In vitro* PTX release profiles of PTX-S-PTX NVs in cell lysates of HeLa cells.

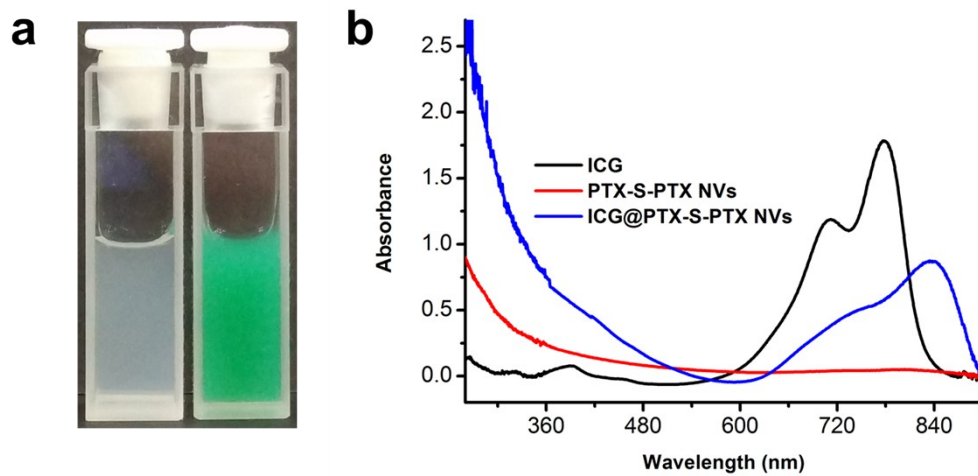


Fig. S14 (a) The photo of PTX-S-PTX NVs (left) and ICG@PTX-S-PTX NVs (right).

(b) UV-vis absorption spectra of ICG, PTX-S-PTX NVs and ICG@ PTX-S-PTX NVs in deionized water.

1. M. C. A. Stuart, J. C. van de Pas and J. B. F. N. Engberts, *J. Phys. Org. Chem.*, 2005, **18**, 929-934.
2. R. Lin, A. G. Cheetham, P. Zhang, Y.-a. Lin and H. Cui, *Chem. Commun.*, 2013, **49**, 4968-4970.